

Numerical analysis to investigate the effect partially filled of porous media inserted in a square channel for different locations

Sarmad A. Ali*, Suhad A. Rasheed

Department of Mechanical Engineering, University of Technology, Baghdad, Iraq

(Communicated by Zakieh Avazzadeh)

Abstract

Various methods are used to improve the heat transfer coefficient of fluids flow inside the various cross-sections of channels, and one of these methods is the use of porous media (PM) in various engineering and industrial applications such as heat exchangers and storage tanks for solar energy. This research paper shows a numerical study using the COMSOL Multiphysics 6.0 program, the effect of the PM (Glass Spheres) inside a square-shaped channel (12 * 12 cm²) by taking three different locations of the PM for two cases (constant heat flux, and constant wall temperature) at the lower surface of a test section and knowing their effect on the distribution of temperature, and velocity to compare them with the absence of the PM for the same channel. The results showed the best temperature distribution to get the best heat transfer coefficient and thus increase the Nusselt number in position (1) of the PM for the test section.

Keywords: Numerical Simulation, Partially Filled, Different Locations, Porous Media, Square Channel
2020 MSC: 94C60

1 Introduction

Recently, the flow of fluids through PM has been widely utilized in most industrial applications to improve the heat transfer process. The most important of these applications are heat exchangers, air conditioning systems, and gas and liquid transport pipes in thermal and gas power plants. Where in this research, a model is designed for a channel in which the type of flow is internal and two-dimensional, and the momentum, energy, and mass equations are solved using COMSOL Multiphysics 6.0 program to find out the effect of the PM on the temperature distribution and velocity during the test section of the channel using water as a fluid and turbulent flow within this application. Many researchers presented in their investigations the flow of fluids and the transfer of heat within the channels of different sections to improve the heat transfer coefficient and thus increase the number of Nusselt. P. C. Huang, and K. Vafai. [5] The study in this article gives a thorough analysis of forced convection augmentation in a channel employing several emplaced porous blocks. To define the flow field inside the porous sections and take into consideration both the inertia effects and the viscous effects, the Brinkman Forchheimer-extended Darcy model is employed. Using a stream function-vorticity technique, the coupled governing equations for the porous/fluid composite system are solved. The presentation and discussion of significant fundamental and practical achievements. These findings provide a complete analysis of the

*Corresponding author

Email address: me.21.06@grad.uotechnology.edu.iq (Sarmad A. Ali)

relationship between the Reynolds, Darcy, Prandtl, inertial, and two crucial geometric parameters which define the problem and the streamline, isotherm, and local Nusselt number distributions. It is proved that there is an ideal porous matrix after a thorough study of the development and variation of the recirculation brought on by the porous medium. Pei-Xue Jiang, and Ze-Pei Ren [7] Using a numerical model that incorporates the thermal nonequilibrium assumption, the impacts of viscous dissipation, boundary condition assumptions, thermal dispersion, particle sizes, and the variable characteristics of oil are examined in the current research. The outcomes, which are contrasted with the experimental data, demonstrate that the convection heat transfer in PM can be computationally predicted using the thermal non-equilibrium model with the ideal constant wall heat flow boundary condition. Shokouhmand H. et al. [12] This research deals with two cases to investigate the influence of PM on the heat transfer process in a channel with two parallel plates. In the first case, the PM was placed at the end of the two walls of the plate, and the fluid flow was simulated using the Lattice Boltzmann method, where the temperatures were uniform along the wall of the plate. In the second case, the porous medium was placed in the heart of the channel and the results were compared with the first case. Nimvari M. Eshagh et al. [11] The current study uses numerical analysis to examine turbulent flow and heat transmission over a partly porous channel. The center arrangement and border arrangement are two typical configurations of a porous layer in the channel that are taken into consideration. For both designs, various values of the porous layer thickness and the Darcy number are investigated. At the porous/fluid boundary, the turbulent kinetic energy reaches its maximum. Due to the channeling effect, there is a specific thickness where the Nusselt number is maximum for the center arrangement and least for the outer arrangement. For the Darcy numbers 10^{-2} , 10^{-3} , and 10^{-4} , it is shown that the thickness for the center arrangement that generates the highest Nusselt number is 0.83, 0.88, and 0.9, respectively. The Nusselt number for the boundary arrangement also assumes its minimal value at thicknesses between 0.6 and 0.7, with the thickness value at which the minimum Nusselt number occurs increasing with decreasing Darcy number. Chengzhi Hu et al. [4] With the use of the computational fluid dynamics (CFD) approach, an open-Kelvin model also known as a sphere-subtraction model or a pillar model has been developed in this study to examine the heat transfer properties of porous media with high porosity throughout a velocity range of (4 - 90 m/s). The findings showed that pressure drop, heat transfer coefficient, and volumetric heat transfer coefficient all rise with CPI (Cells Per Inch) and fall with increasing porosity. Yuan Yi et al. [17] Concerning thermally evolving forced convective flow in a channel filled with a fluid-saturated PM that is exposed to steady heat flux and local thermal non-equilibrium, analytical and numerical research has been undertaken. The Darcy number, Biot number, effective thermal conductivity ratio, and Graetz number were all combined to affect the longitudinal thermal development in a channel filled with a very porous media. This impact was investigated using the Brinkman-extended Darcy model. The entrance developing region, transition region, and fully developed region are the three distinct thermal regions that can exist along a channel's longitudinal coordinate, and they can all be distinguished using the 3D convective regime maps proposed in this study. These regions can be distinguished based on the relative thicknesses of the fluid and solid thermal boundary layers. Syrine Khadrawi et al. [8] To solve the equations relating to motion and energy for mixed convection, the Darcy-Brinkman model was adopted, and the volume control approach was used. The theoretical study for this research involved numerically simulating mixed convection in a horizontal channel under the sun that contained an incompressible liquid and was partially filled with metallic foam blocks. The Rayleigh number, thermal conductivity ratio, and porosity were the main factors that were the subject of this study's attention. Jalal M. Jalil, and Shrooq J. Ali [6] A double-pass solar air heater's bottom channel was used as a PM for an experimental examination of the thermal efficiency of stainless-steel mesh and steel wool. For a test setup, plans and preparations were made. The heat conductivity of several PM types with varied porosities has been studied. The effects of the thermal conductivity of PM, mass flow rate, and radiation intensity have all been studied. Bilal J. Kkihlefa et al. [9] Experimental research was done to determine the impact of convection heat transfer in vertical mini-tubes using PM and solvent CO₂ at supercritical pressure. In experimental research, miniature tubes with a diameter of 5 and 8 mm and a medium porosity of 0.5 are suggested. Bulk fluid, walls that varied in temperature from 33 to 55 °C, and pressures between 8 and 10 MPa made up the experimental settings. 1750 to 21000 for the Reynolds number, 0.5 to 4.5 Kg/h for the mass flow rate, and 32500 to 110000 W/m² for the heat flux, respectively. Sabah R. Mahdi, and Suhad A. Rasheed, [10] Convection heat transfer has been investigated in a PM-filled, unfilled triangular channel heated proportionally with a constant heat flux (1.3 kW/m²) at the Reynolds number range (3165-10910) with packed beds. In this paper, PM are experimentally investigated. The packed duct has a hydraulic diameter of (0.1 m) and (is 1m) long. It is filled with a porous substance that has spherical glass particles of two distinct sizes (5 mm, and 10 mm). The channel's related porosity values are (0.468, and 0.616). The relationship between changes in porosity and Reynolds number, as well as the relationship between increased heat transfer coefficient and local Nusselt number, are examined in this work. Karrar Gh. Fadhala et al. [2] The experimental tests were carried out in a 0.25 m x 0.25 m square channel that was built and had its bottom wall uniformly heated. On the walls, copper foam baffles with a predetermined porosity of 0.95 are fitted. In a staggered design, baffles were alternately fixed on the top and bottom of the walls at a constant height of 0.25 m in between the two following baffles (center to center). Three different

classes of copper foam's pore density were tested experimentally with a window cut ratio of 0.25 and a constant heat flux of 4.4 kW/m² (10, 15, and 20) PPI. Reynolds numbers were in the range of (38000 - 54000). The current study focuses on investigating the fluid flow and heat transfer of a channel of square cross-section partially filled with a PM in three different locations to compare it with an empty channel. Two cases were used, the first is the lower surface of the test section exposed to uniform heat flux, and the second case is exposed to a constant temperature because both of these parameters have an effect on the heat transfer coefficient by forced convection.

2 The Assumptions in this Work

Water is the working fluid in the current project. The following flow characteristics are so assumed:

- Steady-state (no time).
- Incompressible fluid (ρ is constant).
- Newtonian flow.
- Non-equilibrium.
- No-slip velocity exists between liquid and solid particles when they are in thermal equilibrium.
- No heat generation.
- Single-face flow (water only)
- Two dimensions Cartesian coordinate system (X, Y).
- Turbulent flow (k- ϵ).
- Constant heat flux on the lower surface of the test section.
- The transmission of radiation heat is minimal.

3 Physical Properties of PM

The porous material has many physical and thermal properties that are the most important separator between one material and another, including thermal conductivity coefficient, porosity, permeability, density, and specific volume. Among the most important equations that are used to calculate porosity and permeability are as follows [1, 13, 3]:

- The Porosity of PM:

$$\varepsilon = \frac{\text{Total volume} - \text{Volume of solids}}{\text{Total volume}} \quad (3.1)$$

Also, we can calculate the porosity depending on the following equations:

$$\varepsilon = 0.3454 + 11.6985(d_s) \quad (3.2)$$

$$\varepsilon = 0.3754 + 4.744(d_s) \quad (3.3)$$

$$\varepsilon = 0.37206 + 10.395(d_s) \quad (3.4)$$

- The Permeability of PM:

$$K = \frac{D^2 \varepsilon^3}{150(1 - \varepsilon)^2} \quad (3.5)$$

Where;

ε : Porosity of PM;

D: Solid granules diameter (m).

- The density of PM:

$$\rho_s = \frac{M_s}{V_s} \quad (3.6)$$

Where;

ρ_s : Density of PM (kg/m³);

M_s : Mass of PM (kg);

V_s : Volume of PM (m³).

4 Numerical of Model in COMSOL Multiphysics

At high Reynolds numbers, single-phase flows are simulated using the Turbulent Flow, the physics interface can handle compressible flows at low Mach numbers, weakly compressible flows, and incompressible flows (typically less than 0.3). The Reynolds-averaged Navier-Stokes (RANS) equations for momentum conservation and the continuity equation for mass conservation are the equations that the turbulent flow, k- interface solves. With realizability limitations, the traditional two-equation k- model is used to model the impacts of turbulence. Wall functions are used to simulate flow near walls. Analyses that are both stationary and time-dependent can be performed using the Turbulent Flow, interface. The most important component is Fluid Properties, which include the RANS equations as well as the transport equations and offer an interface for describing the fluid material and its properties. The Model Builder automatically adds the Fluid Properties and Initial Values default nodes when this physics interface is added [14].

$$\frac{1}{\varepsilon_p} \rho(u \cdot \nabla) u \frac{1}{\varepsilon_p} = \nabla \cdot [-\rho I + K] - \left(\mu k^{-1} + \beta \rho |u| + \frac{Q_m}{\varepsilon_p^2} \right) u + F \quad (4.1)$$

$$\rho \nabla \cdot u = Q_m \quad (4.2)$$

$$K = \mu \frac{1}{\varepsilon_p} (\nabla u + (\nabla u)^T) - \frac{2}{3} \mu \frac{1}{\varepsilon_p} (\nabla \cdot u) I \quad (4.3)$$

$$\rho(u \cdot \nabla) k = \nabla \cdot \left[\left(\mu + \frac{\mu_T}{\sigma_k} \right) \nabla k \right] + p_k - \rho \epsilon \quad (4.4)$$

$$\rho(u \cdot \nabla) \varepsilon = \nabla \cdot \left[\left(\mu + \frac{\mu_T}{\sigma_\varepsilon} \right) \nabla \varepsilon \right] + C_{\varepsilon 1} \frac{\varepsilon}{k} p_k - C_{\varepsilon 2} \rho \frac{\varepsilon^2}{k}, \varepsilon = \epsilon p \quad (4.5)$$

The dependent variables (fields) for this physics interface are as follows:

- μ : Fluid (water) dynamic viscosity (kg/m. s);
- u : Velocity vector (m/s);
- ρ : Fluid (water) Density (kg/m³);
- P : The pressure (N/m²);
- K : Permeability of the PM;
- Q_m : The mass of the sink.

Also, the equations of heat transfer through a PM:

$$d_z \rho_f C_{p_f} u \cdot \nabla \cdot q = d_z Q + q_o + d_z Q_p + d_z Q_{vd} + d_z Q_{geo} \quad (4.6)$$

$$q = -d_z k_{eff} \nabla T \quad (4.7)$$

$$k_{eff} = \varepsilon_p k_f + \theta_s k_s + \theta_{imf} k_{imf} + k_{disp} \quad (4.8)$$

5 Modeling and Analysis

It is suggested that we investigate the phenomena of forced convection in a channel (square cross-section) with dimensions $(12 * 12 \text{ cm}^2)$ partially filled with the PM in this essay. The stated geometry of the physical issue under study. The dimensions are $L = 0.5 \text{ m}$ and $H = 0.12 \text{ m}$. the input temperature (293.15 K) and the inlet fluid (water) velocity (0.05 m/s) . Additionally, the upper surface is insulated while the bottom surface is constantly exposed for two cases the first is uniform heat flux (1000 W/m^2) , and the second is constant wall temperature (300 K) . In the current study, the Navier-Stokes equations are used to maintain the solution to our issue in the fluid domain, and the Turbulent Flow $k-\omega$ equations are used to simulate the flow in the porous layer. The entire Navier-Stokes equation for fluids or the Turbulent Flow $k-\omega$ model for PM is obtained by maintaining the respective terms in the conservation equations. This suggests that when the permeability contrast is high, there will be challenges with convergence and accuracy in the numerical calculations at the fluid-porous interface (low Darcy number in the porous layer).

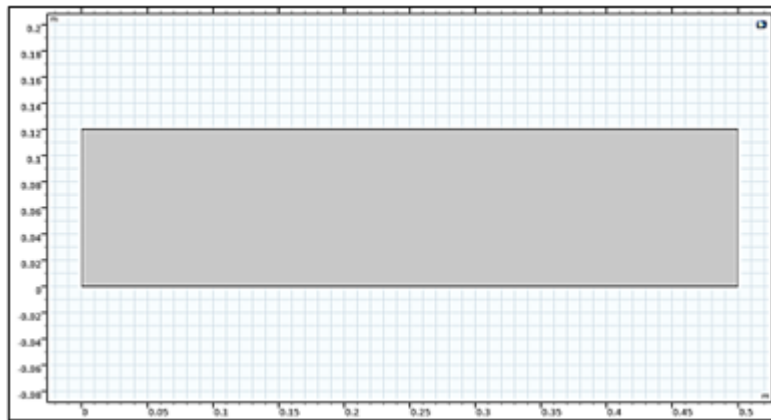


Figure 1: 2D geometry of a channel (test section) devoid of PM

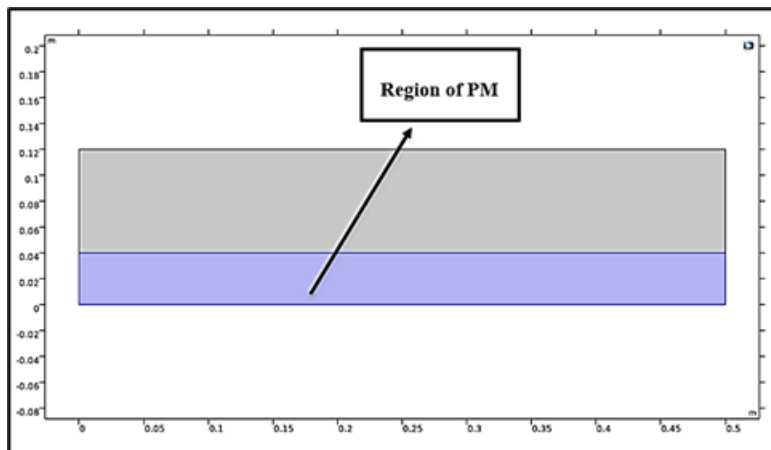


Figure 2: 2D geometry of a channel (test section) for location (1) of a PM

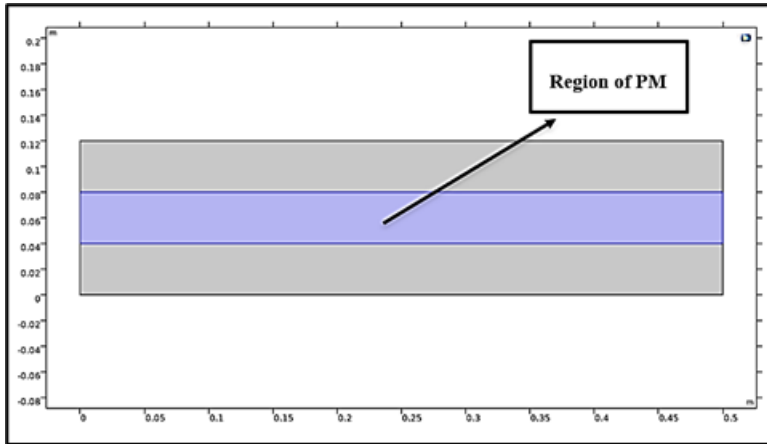


Figure 3: 2D geometry of a channel (test section) for location (2) of a PM

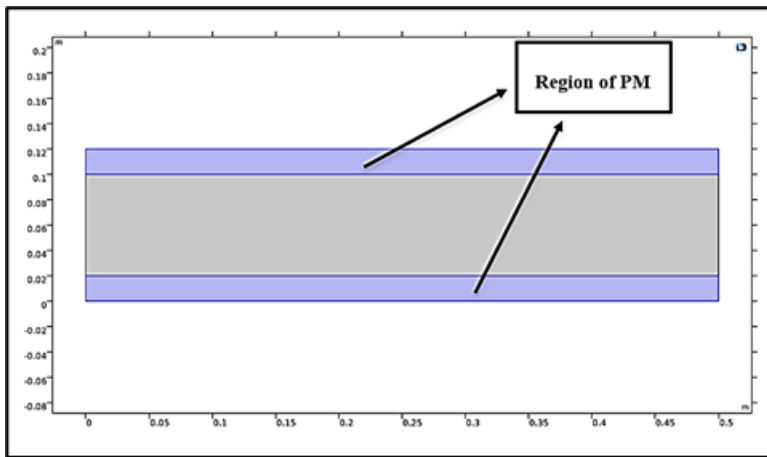


Figure 4: 2D geometry of a channel (test section) location (3) of a PM

6 Creating Mesh

However, COMSOL gives users the option to have a custom-designed mesh for both structured and unstructured types, making meshing practically smooth and "automatic." Mesh files may be imported by users, and the imported mesh can be used to construct geometry [14]. In addition, this program gives us several options for making the mesh in determining the type of element size [Extremely coarse, Extra coarse, Coarser, Normal, Fine, Finer, Extra fine, and extremely fine], The finer type is adapted to solve the numerical analysis of the test section mod. This type of mesh was chosen because it has the values of temperature, speed, and pressure distribution for the test channel, which does not have a big difference, but has become very close to the type before it, which is fine as shown in figures below, also table 1 shows the amount of mesh for the test section of the domain and boundary elements.

Table 1: Mesh size of a channel (test section)

PM	Domain Elements	Boundary Elements
Without	50516	1390
Position 1	49772	1568
Position 2	48462	1746
Position 3	52422	1934

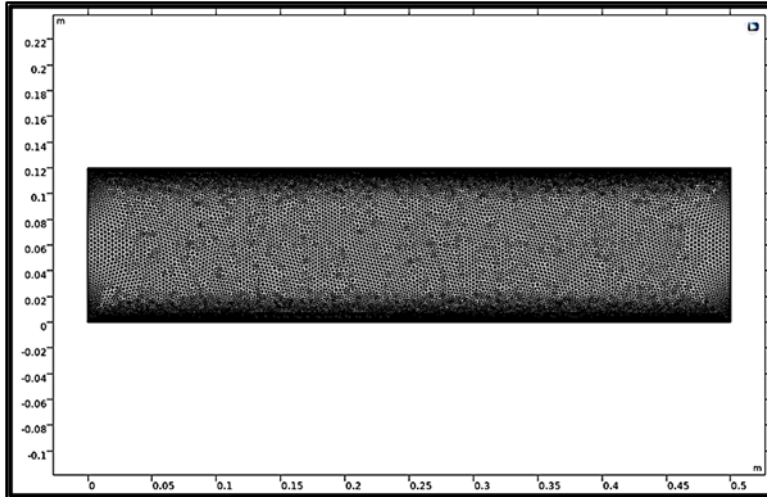


Figure 5: 2D mesh generation of a clear channel (test section)

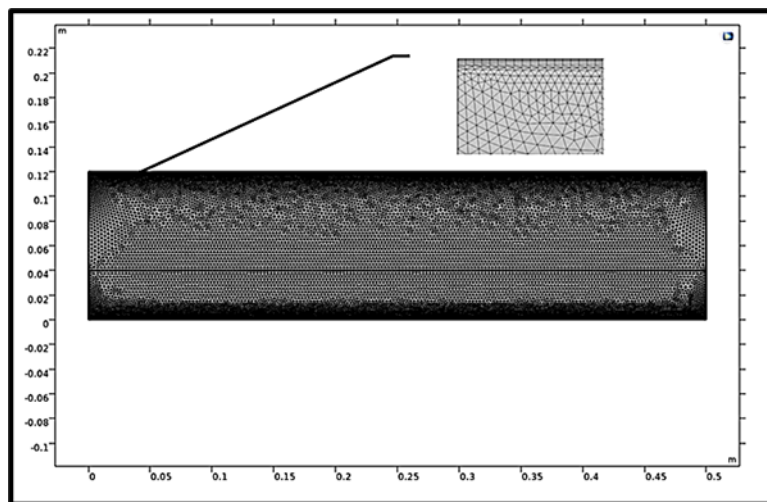


Figure 6: 2D mesh generation of a channel (test section) for location (1) of a PM

7 Governing Equations

The fundamental differential equations for heat transfer and fluid motion, including the conservation of energy, momentum, and mass, are given. One of the most helpful techniques for complex phenomena without turning to expensive prototypes and challenging experimental measurements is computational fluid dynamics (CFD). The temperature profiles are determined using computational fluid analysis. Every equation is displayed in a Cartesian coordinate system.

7.1 Conservation of mass

For an incompressible fluid, steady state, and two-dimensional system, this can be represented analytically [16].

$$\frac{\partial u}{\partial x} + \frac{\partial v}{\partial y} = 0 \tag{7.1}$$

Where;

u: The direction of the velocity around the x-axis.

v: The direction of the velocity around the y-axis.

7.2 Conservation of momentum

The Navier-Stokes equations, which also describe momentum conservation in fluid flow, are another important group of equations that govern fluid flow and are derived from Newton's second law. For an incompressible fluid, the full instantaneous equations for the so-called Darcy-equilibrium equations are as follows [15]:

$$\frac{1}{\varepsilon^2} \left[u \frac{\partial u}{\partial x} + v \frac{\partial v}{\partial y} \right] = -\frac{1}{\rho_f} \frac{\partial p}{\partial x} + \frac{1}{\varepsilon^2} v_{eff} \left(\frac{\partial^2 u}{\partial x^2} + \frac{\partial^2 u}{\partial y^2} \right) - \left[\frac{v_f}{k} + \frac{\varepsilon C}{\sqrt{K}} |\bar{V}| \right] u \quad (7.2)$$

$$\frac{1}{\varepsilon^2} \left[u \frac{\partial u}{\partial x} + v \frac{\partial v}{\partial y} \right] = -\frac{1}{\rho_f} \frac{\partial p}{\partial z} + \frac{1}{\varepsilon^2} v_{eff} \left(\frac{\partial^2 v}{\partial x^2} + \frac{\partial^2 v}{\partial y^2} \right) - \left[\frac{v_f}{k} + \frac{\varepsilon C}{\sqrt{K}} |\bar{V}| \right] v \quad (7.3)$$

Where;

$|\bar{V}|$: absolute velocity with no dimensions;

v_{eff} : Kinematic viscosity that is effective;

C : Constant.

7.3 Conservation of Energy

The formula for the governing equation of non-dimensional energy [15]:

$$u \frac{\partial T}{\partial x} + v \frac{\partial T}{\partial y} = \frac{k_{eff}}{(\rho C p)_f} \left[\left(\frac{\partial^2 T}{\partial x^2} \right) + \left(\frac{\partial^2 T}{\partial y^2} \right) \right] \quad (7.4)$$

8 Results and Discussion

In this part, the results are presented to find out the effect of the presence of the PM inside the channel on the distribution of temperatures and velocities in two cases, the first with the constant of the heat flux below the test section, and the second with the constant temperature of the lower wall by taking different locations of the PM and compared without the presence of the PM of the same test section.

8.1 Distribution of Temperatures for Case (1)

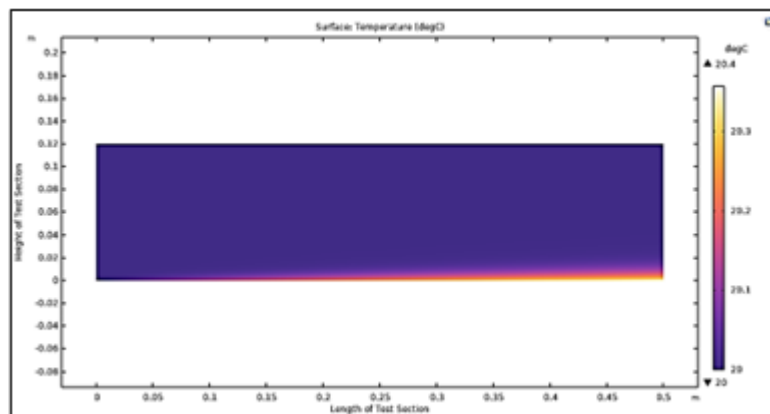


Figure 7: Temperature distribution of a 2D for a clear channel (test section)

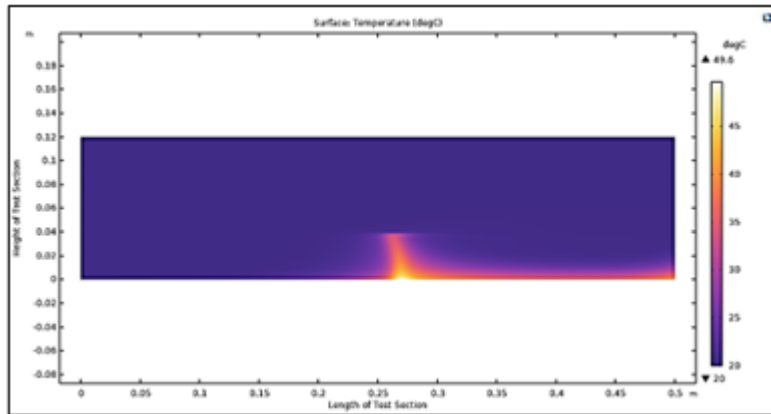


Figure 8: Temperature distribution of a 2D channel (test section) for location (1)

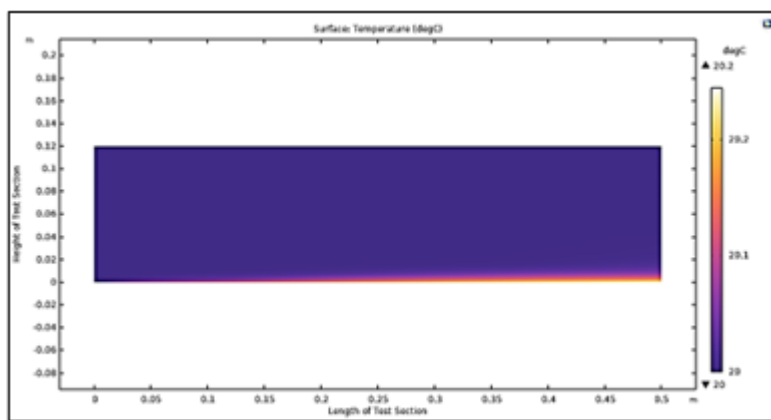


Figure 9: Temperature distribution of a 2D channel (test section) for location (2)

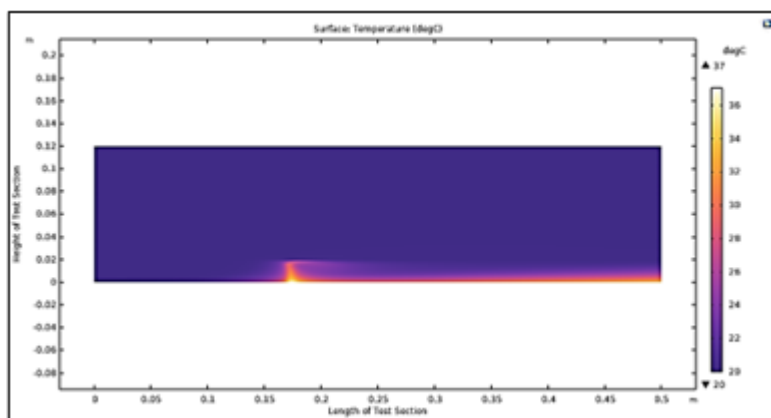


Figure 10: Temperature distribution of a 2D channel (test section) for location (3)

8.2 Distribution of Temperatures for Case (2)

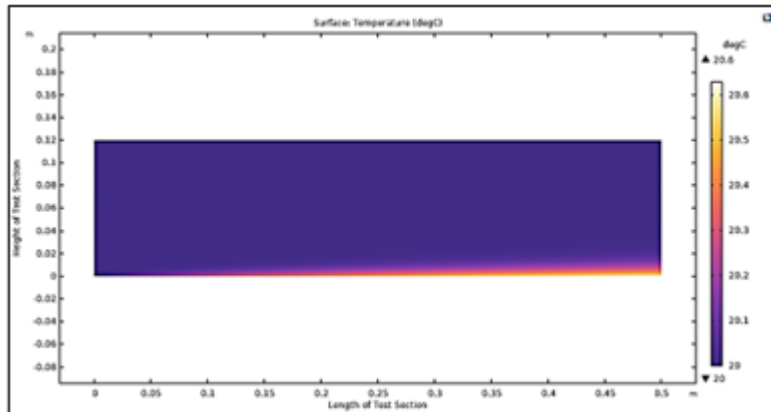


Figure 11: Temperature distribution of a 2D for a clear channel (test section)

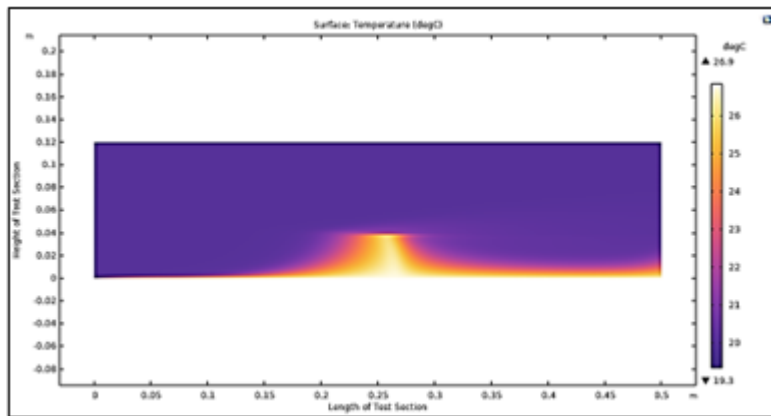


Figure 12: Temperature distribution of a 2D channel (test section) for location (1)

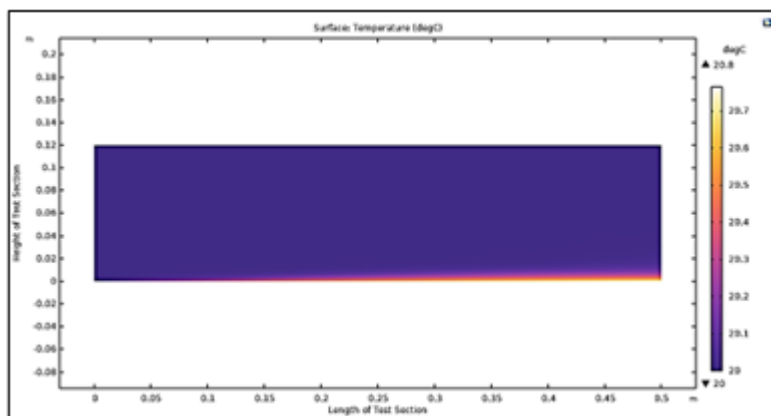


Figure 13: Temperature distribution of a 2D channel (test section) for location (2)

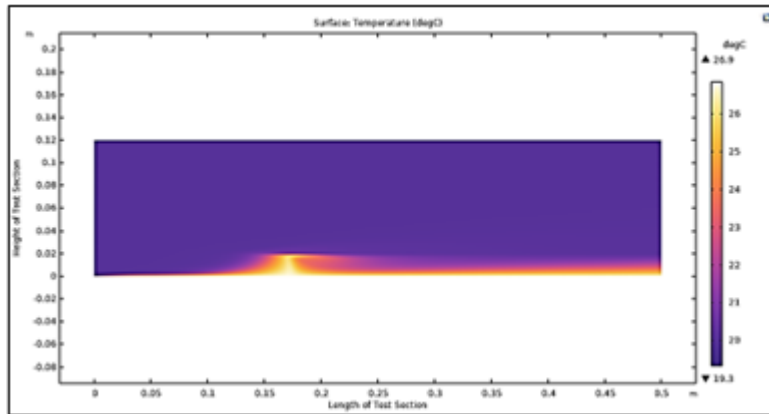


Figure 14: Temperature distribution of a 2D channel (test section) for location (3)

8.3 Velocity Distribution for Cases (1, 2)

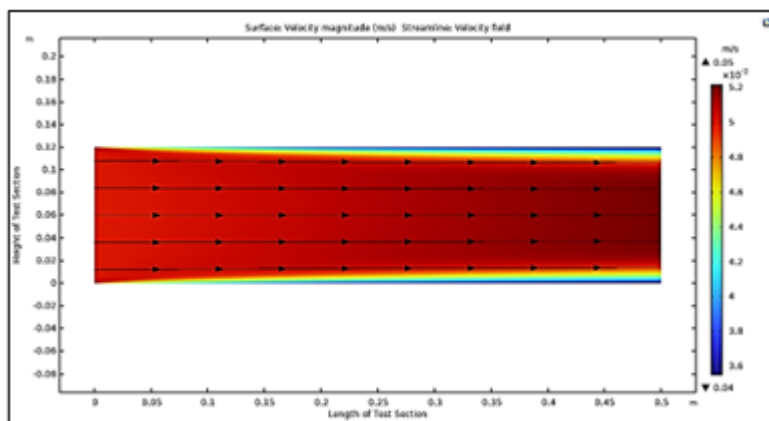


Figure 15: Velocity distribution of a 2D for a clear channel (test section)

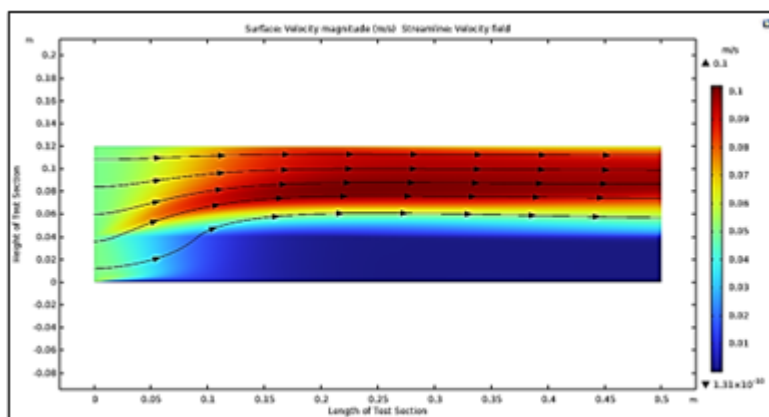


Figure 16: Velocity distribution of a 2D channel (test section) for location (1)

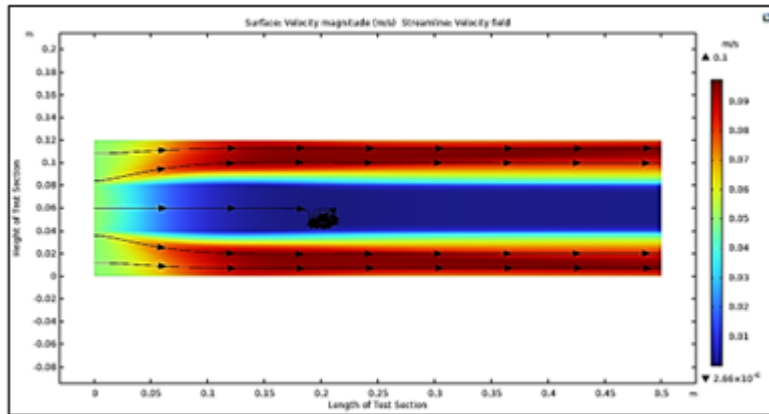


Figure 17: Velocity distribution of a 2D channel (test section) for location (2)

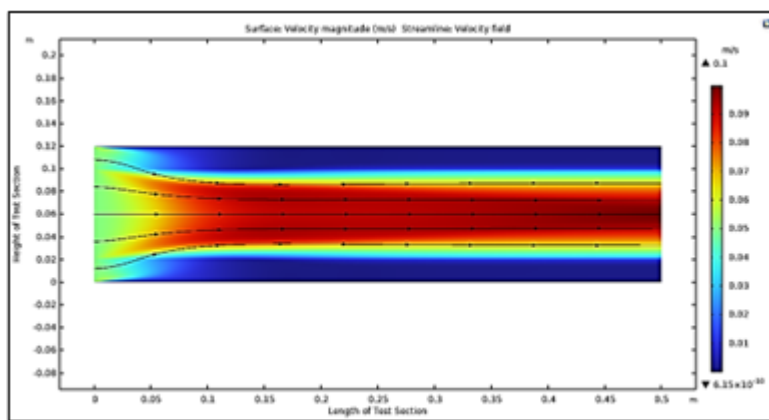


Figure 18: Velocity distribution of a 2D channel (test section) for location (3)

8.4 Temperature and Velocity Profile

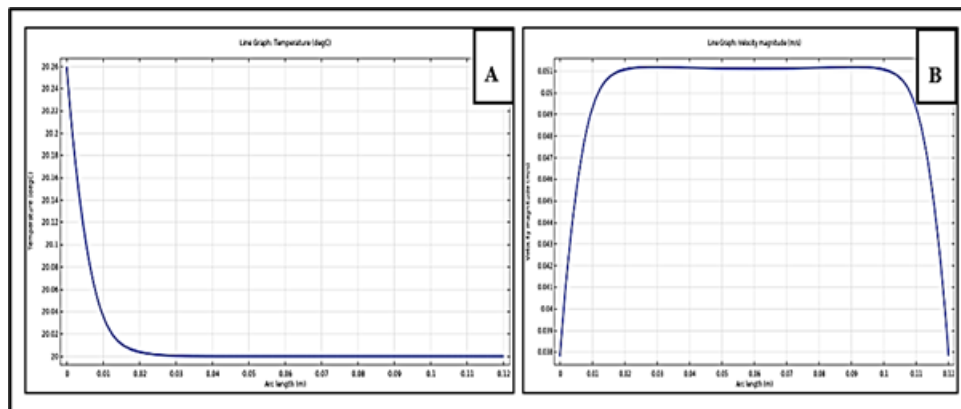


Figure 19: The temperature profile of the test section without PM is shown in (A), and the velocity profile without PM is shown in (B)

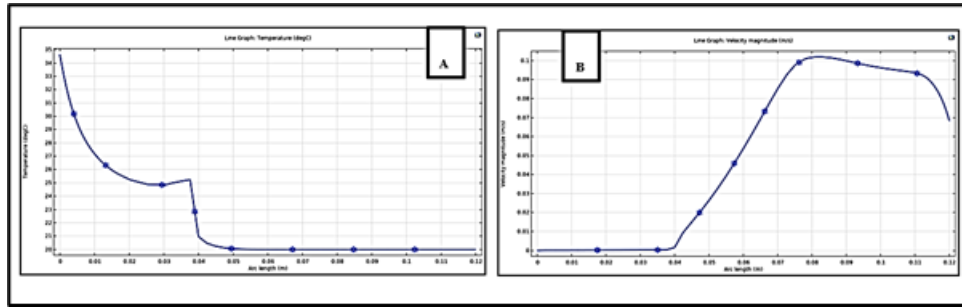


Figure 20: The temperature profile of the test section for a position (1) of PM is shown in (A), and the velocity profile of the test section for a position (1) of PM is shown in (B)

9 Conclusions

1. The presence of the PM improves the heat transfer process and thus increases the Nusselt number and heat transfer coefficient.
2. The presence of PM leads to the deformation of the temperatures and velocity profile.
3. The decrease in the value of permeability affects the increase in the obstruction of fluid movement through the PM.
4. Changing the position of the PM has an important role in the temperature distribution to improve the heat transfer coefficient.
5. The presence of the PM works to increase the velocity gradient of the fluid due to the obstruction that occurs to the fluid flow through the PM.

10 Recommendations

1. Studying the effect of adding hybrid nanofluids on improving the local heat transfer coefficient.
2. Changing the angle of the test section by taking more than one angle and studying its effect on the temperature and velocity distribution.
3. Studying the effect of changing the type of fluid used on the temperature distribution, velocity, local heat transfer coefficient, and local Nusselt number.
4. Changing the location of the heat flux by taking different locations on the test section and studying their effect on the heat transfer process and improving the local heat transfer coefficient and the local Nusselt number.

References

- [1] R. Draby, *Chemical engineering fluid mechanics*, 2 ed., Marcel Dekker, New York, 2001.
- [2] K.Gh. Fadhala, E.M. Fayyadh, and A.. Mohammed, *Effect of copper foam baffles on thermal hydraulic performance for staggered arrangement in a duct*, *Engin. Technol. J.* **41** (2022), no. 1, 243–256.
- [3] K.H. Hilal, *Fluid flow and heat transfer characteristics in a vertical tube packed bed media*, Ph.D. thesis, University of Technology, 2004.
- [4] C. Hu, Y. Zeng, M. Zhang, and H. Zhang, *Numerical simulation on the forced convection heat transfer of porous medium for turbine engine heat exchanger applications*, *Appl. Thermal Engin.* **180** (2020), 115845.
- [5] P.C. Huang and K. Vafai, *Analysis of forced convection enhancement in a channel using porous blocks*, *J. Thermophys. Heat Transfer* **8** (1994), no. 3, 563–573.
- [6] Jalal M. Jalil and Shrooq J. Ali, *Thermal investigations of double pass solar air heater with two types of porous media of different thermal conductivity*, *Engin. Technol. J.* **39** (2021), no. 1A, 79–88.
- [7] P.-X. Jiang and Z.-P. Ren, *Numerical investigation of forced convection heat transfer in porous media using a thermal non-equilibrium model*, *Int. J. Heat Fluid Flow* **22** (2001), no. 1, 102–110.
- [8] S. Kadhrawi, F.S. Oueslati, and R. Bennacer, *Mixed convection in a channel partially filled with metal foam blocks*, *MATEC Web Conf.* **330** (2020).

-
- [9] B.J. Kkihlefa, A.A. Jaddoa, and A.H. Reja, *The influence of convection heat transfers for vertical mini-tubes using solvent carbon dioxide and porous media at supercritical pressure*, Engin. Technol.J. **39** (2021), no. 9, 1409–1419.
- [10] S.. Mahdi and S.A. Rasheed, *Experimental study convection heat transfer inside the triangular duct filled with porous media*, Engin. Technol. J. **41** (2022), no. 1, 203–217.
- [11] M.E. Nimvari, M. Maerefat, and M.K. El-Hossaini, *Numerical simulation of turbulent flow and heat transfer in a channel partially filled with a porous media*, Int. J. Thermal Sci. **60** (2012), 131–141.
- [12] H. Shokouhmand, F. Jam, and M.R. Salimpour, *The effect of porous insert position on the enhanced heat transfer in partially filled channels*, Int. Commun. Heat Mass Transfer **38** (2011), no. 8, 1162–1167.
- [13] A.H.R. Suhad, *Mixed convection heat transfer in saturated porous media inside a circular tube*, Ph.D. thesis, University of Technology, 2006.
- [14] M Tabatabaian, *Cfd module: Turbulent flow modeling*, Mercury Learning and Information, 2015.
- [15] J. Tu, G.-H. Yeoh, and C. Liu, *Computational fluid dynamics: A practical approach*, 3 ed., Elsevier Ltd, United Kingdom, 2018.
- [16] H.K. Versteeg and W. Malalasekera, *An introduction to computational fluid dynamics*, 2 ed., Pearson Education Limited, 2007.
- [17] Y. Yi, C. Ma, C. Ji, and W. He, *Analytical and numerical study on thermally developing forced convective flow in a channel filled with a highly porous medium under local thermal non-equilibrium*, Transport Porous Media **136** (2021), no. 2, 541–567.